Understanding the entanglement entropy and spectra of 2D quantum systems through arrays of coupled 1D chains

PHYSICAL REVIEW B **87**, 241103(R) (2013)

Understanding the entanglement entropy and spectra of 2D quantum systems through arrays of coupled 1D chains

Andrew J. A. James and Robert M. Konik

Condensed Matter Physics & Materials Science Department, Brookhaven National Laboratory, Upton, New York 11973-5000, USA

(Received 28 August 2012; revised manuscript received 10 May 2013; published 18 June 2013)

We describe an algorithm for studying the entanglement entropy and spectrum of two-dimensional (2D) systems, as a coupled array of N one-dimensional chains in their continuum limit. Using the algorithm to study the quantum Ising model in 2D (both in its disordered phase and near criticality), we confirm the existence of an area law for the entanglement entropy and show that near criticality there is an additive piece scaling as $c_{\text{eff}}\ \log(N)/6$ with $c_{\text{eff}} \approx 1$. Studying the entanglement spectrum, we show that entanglement gap scaling can be used to detect the critical point of the 2D model. When short-range (area law) entanglement dominates we find (numerically and perturbatively) that this spectrum reflects the energy spectrum of a single quantum Ising chain.

DOI: 10.1103/PhysRevB.87.241103 PACS number(s): 75.10.Jm, 03.67.Mn, 05.30.−d, 64.70.Tg

In the past decade concepts borrowed from information theory have become important tools in analyzing the properties of many-body quantum systems.[1] The preeminent quantity in this regard is the bipartite entanglement entropy S_E. This measure of nonlocal quantum entanglement can be used to characterize quantum critical points,[2–4] access hidden topological order,[5–8] and provides a simple measure for the applicability of the density matrix renormalization group (DMRG), one of the most commonplace numerical techniques in low dimensions.[3,9,10]

Most is known about S_E in one spatial dimension (1D). In 1D S_E signals the onset of criticality through an associated universal logarithmic divergence with system size L.[2,4] Both the coefficient of this divergence (i.e., the central charge of the theory's conformal algebra) and its subleading corrections in L (determining the theory's operator content[11,12]) serve to uniquely specify the underlying critical theory.

There is less certainty above 1D. Regardless of criticality, S_E possesses a term scaling as the area of the boundary separating the bipartite region.[13] Beyond this "area law" term, there can be subleading, universal contributions to S_E. Generalizing the results in 1D, the anti-de Sitter/conformal field theory correspondence suggests that S_E in all odd spatial dimensions will be characterized by universal logs.[14,15] Universal terms have also been argued for in the set of theories in two dimensions (2D) known as conformal quantum critical points (CQCP)[7,16–21] as well as systems with spontaneously broken symmetries.[22–25] Recent studies of gapless states on the torus[21,26,27] have confirmed the existence of apparently universal terms that depend on system shape.

In this Rapid Communication we demonstrate an algorithm for investigating the behavior of S_E in 2D systems. The algorithm works by treating the model in an anisotropic limit as a mixture of continuum and discrete degrees of freedom, making it amenable to a 1D-like DMRG algorithm. A major strength of the DMRG approach is that it works directly with the eigenvalues of the reduced density matrix ρ_r, the distribution of which governs the entanglement content. This allows us to simultaneously probe a variety of entanglement measures in 2D. Alternative techniques, such as quantum Monte Carlo, that do not have direct access to ρ_r, are more restricted.

As a case study, we consider the quantum Ising model (or transverse field Ising model) in two spatial dimensions: a paradigmatic model for strongly correlated physics. We find that S_E in 2D shares a number of characteristics with 1D—including logarithmic scaling at criticality, in agreement with other studies[21,26,27]—and propose a scaling form to explain our results.

Furthermore, we analyze the entanglement spectrum (ES). While the ES was first studied as a means to understand the efficacy of the DMRG algorithm[28–30] and then as a means of detecting topological order,[31] it is now explored in nontopological systems in attempts to elucidate a connection between it and an excitation spectrum.[32–36] We find that the scaling of the entanglement spectrum can be used to detect the critical point of the 2D system (a significant numerical advantage over calculating the energy gap), a result previously suggested only in 1D.[37,38]

Model and DMRG algorithm. We study the 2D quantum Ising model as a set of 1D quantum Ising chains (QICs), each with periodic boundary conditions and of length R, coupled through their spin operator:

$$H = \sum_i H_i^{\text{1D QI}} + J_\perp \sum_{\langle ij \rangle} \int_0^R dx\, \sigma_i(x)\sigma_j(x), \qquad (1)$$

where i is a sum over chain index. The Hamiltonian $H_i^{\text{1D QI}}$ is taken in its continuum limit, that of a massive Majorana fermion, $H_i^{\text{1D QI}} = \int dx (i\bar{\psi}\partial_x\bar{\psi} - i\psi\partial_x\psi + i\Delta\bar{\psi}\psi)$, where $\bar{\psi}/\psi$ are right- and left-moving components of the Majorana fermion. In lattice notation, $H^{\text{1D QI}} = -J\sum_j \sigma_j^z\sigma_{j+1}^z + (g+1)\sigma_j^x$, and we identify $\sigma^z \to \sigma$, $\Delta = gJ$. In this Rapid Communication we focus on systems built from chains with negative mass ($\Delta < 0$), as in this case one can drive the system to the critical point by increasing the magnitude of the interchain coupling $J_\perp$ (see Fig. 1). We employ a DMRG algorithm adapted to studying coupled 1D chains as described in Ref. 39, treating individual chains as equivalent to individual lattice sites in a conventional DMRG algorithm. As with

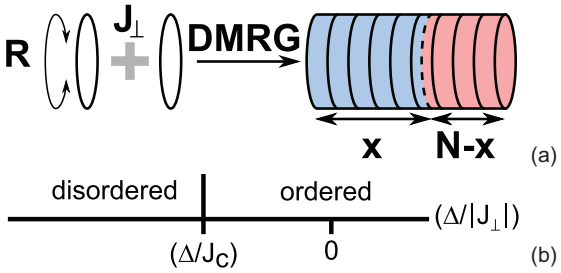

FIG. 1. (Color online) (a) An array of continuum chains of length R, with interchain coupling $J_\perp$. Each chain is a single site in our DMRG algorithm. (b) The phase diagram of coupled QICs.

all DMRG algorithms, this allows us to readily extract the entanglement entropy and spectrum.

This methodology is based in part on the truncated spectrum approach (TSA) to studying perturbed conformal and integrable field theories.[40] In the TSA the underlying conformal or integrable theory provides a particularly apt basis in which to study relevant (in the renormalization group sense) perturbations. With such perturbations, the low energy sector of the full theory can be understood as a mixing of the low energy sector of the unperturbed theory (even if the two energy spectra are dramatically different). Thus the high energy part of the theory can be neglected by imposing an energy cutoff or taken into account in a variational scheme borrowed from the numerical renormalization group.[41] In the following we use a cutoff Λ on the chains.

As with perturbations in the TSA, our DMRG trades on the ability to compute matrix elements of the interchain coupling exactly, i.e., $\langle s|\sigma_j\sigma_{j+1}|s'\rangle$, where $|s\rangle,|s'\rangle$ are two states on a pair of neighboring chains. Using integrable or conformal 1D chains means we are able to incorporate much of the strongly correlated physics before the numerical analysis has even begun.

DMRG algorithms in 2D are limited relative to 1D because S_E grows with the length of boundary between blocks (in this implementation, R, the chain length).[9,10] Approaching the thermodynamic limit then requires extrapolation and judicious choices of aspect ratio and boundary conditions.[42] Our use of continuum chains plays an important role in allowing the DMRG algorithm to work successfully. In continuum field theories, the finite size errors are exponentially suppressed in system size R.[43] This means that the chains can be in the thermodynamic limit for certain quantities, even for comparatively small R.[44] Keeping R small allows for smaller S_E and hence an efficient DMRG implementation. As a corollary to this we find we need to keep comparatively few eigenstates of the reduced density matrix, ranging from tens deep in the ordered phase to $\sim$200 close to the critical point in order to obtain truncation errors on the order of 10^{-5} (for additional details see Ref. 44). Thus while the Hilbert space of the individual sites (i.e., the chains) can involve many hundreds of states, we need to keep far fewer states from the reduced density matrix.

The algorithm has been shown to successfully analyze various conventional properties of large arrays of coupled QICs.[39] It was able to reproduce the scaling form (in terms of the dimensionless combination $J_\perp^{4/7}\Delta^{-1}$) of the first excited gap in the disordered phase. For this system it is possible to analytically compute the finite chain R corrections, and an excellent match with the DMRG numerics was found. Most significantly, the exponent ν governing the vanishing of the mass gap Δ_{2D} as the critical coupling is approached, i.e., $\Delta_{2D} \sim |J_\perp - J_c|^\nu$, was computed. It was found to be $\nu = 0.622 \pm 0.019$, in good agreement with the accepted value $\nu = 0.630$ and with a tensor based method,[45,46] for the three-dimensional classical Ising model, demonstrating that the method successfully captures the physics of the 2D quantum system.

Entanglement entropy. We couch our results for S_E in terms of a scaling form applicable in the vicinity of criticality. This scaling form must take into account the universal and the nonuniversal (i.e., cutoff Λ dependent) contribution to the area law as well as a subleading universal logarithmic contribution that we believe we have detected in our numerics. We allow this logarithm to be dependent on the system aspect ratio (akin to that for 2D CQCP[21])—a necessity if we insist on matching perturbation theory away from criticality. The scaling form we adopt is then

$$S_E = \alpha R\Lambda + \frac{c}{6}\log\frac{N}{|\Delta|R} + \frac{R}{\xi_\parallel} f\left(\frac{N}{\xi_\perp}, \frac{R}{\xi_\parallel}, \frac{\xi_\perp}{|\Delta|\xi_\parallel}\right), \quad (2)$$

where α is a nonuniversal constant, $\xi_\parallel$ and $\xi_\perp$ are the correlation lengths parallel and perpendicular to the chains, respectively, and f is a scaling function. This form is chosen so that near criticality, where the scaling function is $f(0,0,\text{const.})$, we obtain

$$S_E \sim \alpha R\Lambda + \frac{c}{6}\log\frac{N}{|\Delta|R} + \text{const.} \quad (3)$$

Here Δ serves as an effective inverse lattice spacing. Far from criticality a perturbative calculation[44] shows

$$S_E = \frac{1}{8}\frac{|\Delta|R}{\xi_\perp}\exp\left(-2\frac{|\Delta|\xi_\parallel}{\xi_\perp}\right), \quad (4)$$

indicating that the nonuniversal contribution has vanished (i.e., $\alpha = 0$) and that in this limit we can identify $f \sim -(c\xi_\parallel/6R)\log[N/(|\Delta|R)] + g[\xi_\perp/(|\Delta|\xi_\parallel)]$.

In presenting our numerical results we start with disordered chains $\Delta = -1$, $\Lambda = 8.0$ and display in Fig. 2 the behavior of

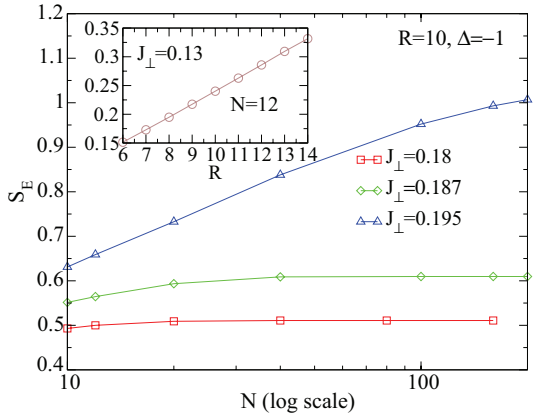

FIG. 2. (Color online) S_E as a function of the number of chains N in the disordered phase and near criticality. Inset: S_E for the same phase as a function of R, the chain length.

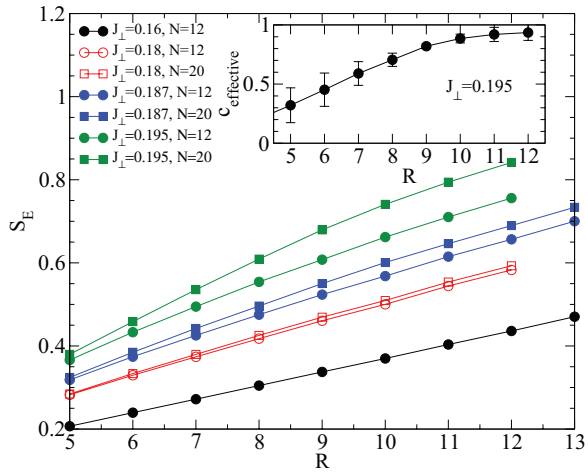

FIG. 3. (Color online) S_E closer to criticality for a block of length $N/2$ as a function of the chain circumference R. For $J_\perp = 0.187$ and 0.195 the data sets are improved using truncation error extrapolation. Inset: The effective value of c extracted. A power-law fit for $R > 7$ yields $c(R) = 1.04(5) - [R/5.4(2)]^{-3.0(7)}$.

S_E as a function of $J_\perp, R$, and N, both deep in the disordered phase and close to criticality. At very small $J_\perp$, S_E displays an area law $S_E \sim R$ as expected, and is nearly constant with N for values greater than ∼10. On increasing $J_\perp$ with fixed R, the value of N at which S_E saturates increases, and eventually a logarithmic dependence on N becomes evident. At $J_\perp = 0.195$, $R = 10$ this $S_E \sim \log N$ behavior extends up to systems of $N \sim 100$.

In Fig. 3 we show the emerging $\log N$ behavior as a function of R. For $J_\perp = 0.187, 0.195$ the gradient becomes N dependent, indicating a crossover as $\xi_\perp$ grows. Also visible is a crossover with R between limiting forms of f. At these values of $J_\perp$ we find considerable improvement in our results on performing truncation error extrapolation,[47] to compensate for the effect of the maximum DMRG correlation length.[42,48] For $J_\parallel = 0.195$, where the logarithm behavior extends over the largest range, we can subtract Eq. (3) at varied N and fixed R to estimate c. Using data for $N = 4$, 12, and 20 we find the behavior in the inset of Fig. 3: the extracted value of c tends to a constant for large R. A power-law fit yields $c \to 1.04(5)$.

Prompted by the logarithmic piece and in analogy with the 1D case, we look for "chord" scaling near criticality:

$$S_E = \frac{c}{6} \log \left[\sin \left(\frac{\pi x}{N} \right) \right] + \cdots . \tag{5}$$

In our DMRG calculations x corresponds to the number of chains in the "system" block, while there are $N - x$ chains in the "environment" block (Fig. 1). In Fig. 4 we plot S_E versus the "chord length" at $J_\perp = 0.195$ for a variety of aspect ratios; there is a clear linear relation. The extracted values of c are given in Table I. Similar scaling behavior in 2D was observed in Ref. 27 although recent analytical results for 2D CQCPs[21] suggest that for 2D CQCPs this chord scaling is merely an excellent first approximation.

Entanglement spectra. In principle, much more information is encoded in the full spectrum of the reduced density matrix ρ_r than in the number $S_E = -\mathrm{Tr}\, \rho_r \log \rho_r$ alone. The ES

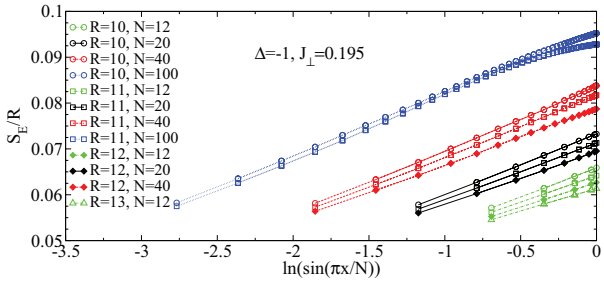

FIG. 4. (Color online) S_E/R for $J_\perp = 0.195$ as a function of block length.

is usually defined in terms of a fictitious Hamiltonian $\rho_r = \exp(-H_E)$ so that the ES "energies" are $\omega = -\log \rho_r$. We first consider the entanglement "gap" Δ_{ES}, the difference between the two lowest lying values of the ES. In Refs. 37 and 38 it was proposed that ES scaling in 1D can detect critical points. However, these works do not find agreement with the scaling relation found by Calabrese and Lefevre[49,50] for a 1D conformal system of finite length N, $\Delta_{\mathrm{ES}} \sim \text{const.}/\log(N/\pi)$.[49,50]

In Fig. 5 we plot $\Delta_{\mathrm{ES}} \log(N/\pi)$ against $J_\perp$ for a variety of 2D systems with the same aspect ratio (R/N) but different sizes. Tellingly, the curves cross at a single point $J_c = 0.186(2)$ indicating that we can use this finite size scaling of the entanglement spectrum to discern the critical point of the 2D system. To support this claim we also perform finite size scaling on the true energy gap $(E_1 - E_0)$ in our system (right panel of Fig. 5) and find $J_c = 0.185(2)$. This also agrees well with the renormalization group improved value $J_c = 0.184(3)$ in Ref. 39. We note that calculating $E_1 - E_0$ is considerably more difficult than Δ_{ES}, as the former requires targeting the first excited state with the DMRG algorithm. Using Δ_{ES} to find J_c therefore offers a significant numerical advantage.

Finally, we consider the ES as a function of the momentum k along the chain direction. It has been shown that the ES of spin ladders closely resembles the true energy spectrum of a single spin chain.[32–34] The spectrum of the QIC separates into two sectors: Neveu-Schwarz (NS) and Ramond (R).[44] For a $\Delta < 0$ chain these correspond to even and odd numbers of solitons along the chain, respectively. Similarly the ES splits into two sectors, depending on whether the state has an even or odd number of chains in the NS sector (assuming $N/2$ is even). Figure 6 shows that at $J_\perp = 0.13$, far from criticality and where short-range (area law) entanglement at the boundary dominates, the low-lying ES resembles that of a single QIC, where the one- and two-soliton sectors are mimicked by ES states with odd and even numbers of NS

TABLE I. Values of c from data in Fig. 4.

	R			
N	10	11	12	13
12	0.76	0.76	0.77	0.77
20	0.78	0.80	0.83	
40	0.80	0.84	0.87	
100	0.80	0.86		

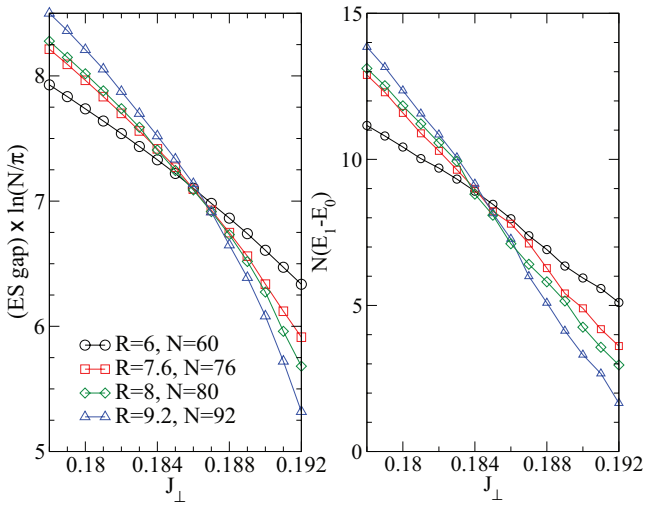

FIG. 5. (Color online) Finite size scaling of both (left) the entanglement gap and (right) the real gap for DMRG calculations in which eigenvalues of ρ_r are kept if they are $\geqslant 5 \times 10^{-7}$.

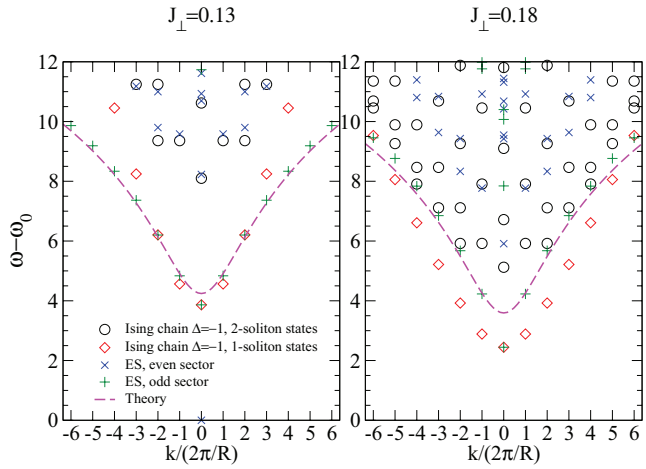

FIG. 6. (Color online) Plot of the entanglement spectra both away from criticality (left), $J_\perp = 0.13$ and closer to criticality (right), $J_\perp = 0.18$. $N = 160$. In both cases the ES is measured relative to its lowest eigenvalue. The two sectors of the energy spectrum of a QIC are also plotted, rescaled so that the lowest band overlaps the lowest ES band at $k = 0$. The curve labeled "theory" is a perturbative calculation in Ref. 44.

chains. Closer to criticality, at $J_\perp = 0.18$, the ES does not resemble that of a disordered QIC, in particular, $\Delta_{\rm ES} \to 0$. A perturbative calculation for weak intrachain coupling gives $\omega = 2\ \log(\Delta^2 + k^2) + \text{const.}$ for the lowest "band" in the ES (see Ref. 44). The good agreement between this prediction (with $\Delta = -1$) and the $J_\perp = 0.13$ spectrum is shown in Fig. 6.

The 1D-like features that we see in our 2D system suggest the following interpretation. Using the intuition that comes from our anisotropic treatment of a 2D system, any 2D system can be thought of as a set of coupled continuum chains. At a critical point, this anisotropic representation does not affect the critical properties (provided the critical point is a point and not a line where a lattice vs continuum treatment might control where along the line one ends up). If at the 2D critical point, a finite number of chains become critical with the remaining chains massive with a gap of at least $\Delta_{\rm min}$, one would expect to see 1D scaling.

In summary, we have shown that an unconventional DMRG technique can be used to study the entanglement content of strongly correlated 2D quantum systems. Using this technique we have established the existence of an additive logarithmic piece in S_E with a universal coefficient $c \approx 1$ for the 2D quantum Ising model. We have also shown that the ES gap can be used to efficiently find a critical point in 2D and that when this gap is large and short-range entanglement is dominant, the ES reflects the spectrum of a single Ising chain.

Acknowledgments. This research was supported by the US Department of Energy (DE-AC02-98CH10886). We are grateful to P. Calabrese, F. Essler, J.-M. Stéphan, and P. Fendley for helpful discussion and for the hospitality of the Galileo Galilei Institute at which part of this work was completed.

[1] L. Amico, R. Fazio, A. Osterloh, and V. Vedral, Rev. Mod. Phys. **80**, 517 (2008).
[2] C. Holzhey, F. Larsen, and F. Wilczek, Nucl. Phys. B **424**, 443 (1994).
[3] G. Vidal, J. I. Latorre, E. Rico, and A. Kitaev, Phys. Rev. Lett. **90**, 227902 (2003).
[4] P. Calabrese and J. Cardy, J. Stat. Mech.: Theory Exp. (2004) P06002.
[5] A. Kitaev and J. Preskill, Phys. Rev. Lett. **96**, 110404 (2006).
[6] M. Levin and X. G. Wen, Phys. Rev. Lett. **96**, 110405 (2006).
[7] E. Fradkin and J. E. Moore, Phys. Rev. Lett. **97**, 050404 (2006).
[8] H.-C. Jiang, Z. Wang, and L. Balents, Nat. Phys. **8**, 902 (2012).
[9] U. Schöllwock, Rev. Mod. Phys. **77**, 259 (2005).
[10] K. A. Hallberg, Adv. Phys. **55**, 477 (2006).
[11] S. Furukawa, V. Pasquier, and J. Shiraishi, Phys. Rev. Lett. **102**, 170602 (2009).
[12] P. Calabrese, M. Campostrini, F. Essler, and B. Nienhuis, Phys. Rev. Lett. **104**, 095701 (2010).
[13] J. Eisert, M. Cramer, and M. B. Plenio, Rev. Mod. Phys. **82**, 277 (2010).
[14] S. Ryu and T. Takayanagi, Phys. Rev. Lett. **96**, 181602 (2006).
[15] T. Nishioka, S. Ryu, and T. Takayanagi, J. Phys. A: Math. Theor. **42**, 504008 (2009).
[16] J. M. Stéphan, S. Furukawa, G. Misguich, and V. Pasquier, Phys. Rev. B **80**, 184421 (2009).
[17] M. Oshikawa, arXiv:1007.3739.
[18] M. P. Zaletel, J. H. Bardarson, and J. E. Moore, Phys. Rev. Lett. **107**, 020402 (2011).
[19] J. M. Stéphan, G. Misguich, and V. Pasquier, Phys. Rev. B **84**, 195128 (2011).
[20] B. Hsu, M. Mulligan, E. Fradkin, and E.-A. Kim, Phys. Rev. B **79**, 115421 (2009).
[21] J.-M. Stéphan, H. Ju, P. Fendley, and R. G. Melko, New. J. Phys. **15**, 015004 (2013).
[22] O. A. Castro-Alvaredo and B. Doyon, Phys. Rev. Lett. **108**, 120401 (2012).

[23]V. Alba, M. Haque, and A. M. Laüchli, arXiv:1212.5634.
[24]M. Metlitski and T. Grover, arXiv:1112.5166.
[25]M. A. Metlitski, C. A. Fuertes, and S. Sachdev, Phys. Rev. B **80**, 115122 (2009).
[26]L. Tagliacozzo, G. Evenbly, and G. Vidal, Phys. Rev. B **80**, 235127 (2009).
[27]H. Ju, A. B. Kallin, P. Fendley, M. B. Hastings, and R. G. Melko, Phys. Rev. B **85**, 165121 (2012).
[28]K. Okunishi, Y. Hieida, and Y. Akutsu, Phys. Rev. E **59**, R6227 (1999).
[29]M.-C. Chung and I. Peschel, Phys. Rev. B **64**, 064412 (2001).
[30]I. Peschel and V. Eisler, J. Phys. A: Math. Theor. **42**, 504003 (2009).
[31]H. Li and F. D. M. Haldane, Phys. Rev. Lett. **101**, 010504 (2008).
[32]D. Poilblanc, Phys. Rev. Lett. **105**, 077202 (2010).
[33]A. M. Läuchli and J. Schliemann, Phys. Rev. B **85**, 054403 (2012).
[34]J. Schliemann and A. M. Läuchli, J. Stat. Mech.: Theory Exp. (2012) P11021.
[35]V. Alba, M. Haque, and A. M. Läuchli, Phys. Rev. Lett. **108**, 227201 (2012).
[36]I. Peschel and M.-C. Chung, Europhys. Lett. **96**, 50006 (2011).
[37]G. De Chiara, L. Lepori, M. Lewenstein, and A. Sanpera, Phys. Rev. Lett. **109**, 237208 (2012).
[38]L. Lepori, G. De Chiara, and A. Sanpera, Phys. Rev. B **87**, 235107 (2013).
[39]R. M. Konik and Y. Adamov, Phys. Rev. Lett. **102**, 097203 (2009).
[40]V. P. Yurov and Al. B. Zamolodchikov, Int. J. Mod. Phys. A **6**, 4557 (1991).
[41]R. M. Konik and Y. Adamov, Phys. Rev. Lett. **98**, 147205 (2007).
[42]E. M. Stoudenmire and S. R. White, Annu. Rev. Condens. Matter Phys. **3**, 111 (2012).
[43]T. Klassen and E. Melzer, Nucl. Phys. B **362**, 329 (1991).
[44]See Supplemental Material at http://link.aps.org/supplemental/10.1103/PhysRevB.87.241103 for details of the numerics and perturbative calculations.
[45]Z. Y. Xie, J. Chen, M. P. Qin, J. W. Zhu, L. P. Yang, and T. Xiang, Phys. Rev. B **86**, 045139 (2012).
[46]Y. Meurice, Phys. Rev. B **87**, 064422 (2013).
[47]S. R. White and A. L. Chernyshev, Phys. Rev. Lett. **99**, 127004 (2007).
[48]T. Nishino, K. Okunishi, and M. Kikuchi, Phys. Lett. A **213**, 69 (1996).
[49]P. Calabrese and A. Lefevre, Phys. Rev. A **78**, 032329 (2008).
[50]F. Pollmann and J. E. Moore, New J. Phys. **12**, 025006 (2010).